## Title
Root litter decomposition slows with soil depth



## Authors
Pries, Caitlin E Hicks
Sulman, Benjamin N
West, Corinna
et al.

## Publication Date
2018-10-01

## DOI
10.1016/j.soilbio.2018.07.002

Peer reviewed

# Root litter decomposition slows with soil depth

Caitlin E. Hicks Pries[ab] Benjamin N. Sulman[cd] Corinna West[e] Caitlin O'Neill[f] Erik Poppleton[gh] Rachel C. Porras[b] Cristina Castanha[b] Biao Zhu[i], Daniel B. Wiedemeier[j] Margaret S. Torn[b]

## Abstract

Even though over half of the world's soil organic carbon (SOC) is stored in subsoils (>20 cm deep), and the old ages of subsoil OC indicate its cycling differs from surface SOC, there are few studies examining in situ decomposition processes in deep soils. Here, we added $^{13}$C-labeled fine roots to 15, 55, and 95 cm depths of a well-characterized coniferous forestAlfisol and monitored the amount of root-derived C remaining over 6, 12, and 30 months. We recovered the root-derived C in microbial phospholipid fatty acids (PLFAs) after 6 months and in coarse (>2 mm) particulate, fine (<2 mm) particulate, and dense, mineral-associated pools after 6, 12, and 30 months. Overall, root decomposition in the first 6 months was similar among all depths but significantly diverged at 30 months with faster decomposition at 15 cm than at 95 cm. There were more fungal and Gram negative-associated PLFAs at 15 cm than at 95 cm, and $^{13}$C analysis revealed those microbial groups preferred the added root carbon to native SOC. Mineral-associations were not the cause of slower decomposition at depth because similar amounts of applied root C was recovered in the dense fraction at all depths. The largest difference among depths was in the amount of root C recovered in the coarse particulate fraction, which was greater at 95 cm (50%) than at 15 cm (15%). Slower decomposition of the particulate pool at depth likely contributed to the increase in C:N ratios and depletion of $\delta^{13}$C values below 60 cm depth in our soil profiles. Simulations of these soils using the CORPSE model, which incorporates microbial priming effects and mineral stabilization of SOC, reproduced patterns of particulate and mineral-associated SOC over both time and depth and suggested that a lack of priming by root exudates at depth could account for the slower decomposition rate of particulate root material. Decomposition of deep particulate SOC may increase if root exudation or dissolved OC transport to depth increases.

Keywords: Soil organic matter, Carbon, Decomposition, Soil depth, 13C, Fine root, Density fractionation, PLFA

## Introduction

Understanding how decomposition changes with depth is integral to understanding the capacity of deeper soils to store soil organic carbon (SOC) and how vulnerable deeper SOC stocks are to loss due to global change. For instance, if decomposition rates are slower at depth than the surface due to a lack of fresh substrates, then increased plant allocation to roots or shifts in plant community to more deeply-rooted species may increase decomposition. On the other hand, if decomposition rates at depth are

slower due to increased mineral associations or physical protection, SOC stored at depth may be resistant to losses due to global changes like shifting plant communities or warming. However, the processes controlling the cycling of deep SOC have received little attention even though over half of the world's SOC pool is stored below 20 cm (Jobbágy and Jackson, 2000) and long turnover times of deep SOC (Mathieu et al., 2015) imply processes at depth differ from those in the surface soil.

SOC cycling changes with depth because the soil profile is a gradient of interacting biotic and abiotic factors. The majority of plant inputs in the forms of shoot litter, senescent roots, and root exudates are found in the surface soil (<20 cm; Jobbágy and Jackson, 2000; Schrumpf et al., 2013). The lack of inputs to prime microbial activity, such as dissolved organic matter from root exudates or leached litter, can slow decomposition in the subsurface (Fontaine et al., 2007; Kuzyakov, 2010) due to energy (Salomé et al., 2010) or nutrient limitation (Heitkötter et al., 2017). With increasing depth, microbial biomass decreases, and community composition becomes less diverse (Eilers et al., 2012; Fierer et al., 2003; Kramer and Gleixner, 2008). Surface soils also contain more eukaryotes, like fungi (Fierer et al., 2003), arthropods (Petersen and Luxton, 1982), and earthworms (Jiménez and Decaëns, 2000; Lavelle, 1988), which play active roles in bioturbation (Lavelle et al., 2006; Six et al., 2004). At depth, with reduced C inputs and less abundant biota, the influence of soil minerals predominates, leading to a larger proportion of SOM being mineral-associated at depth than at the surface (Angst et al., 2016; Kögel-Knabner et al., 2008; Rumpel et al., 2002; Schrumpf et al., 2013). Microbes compete with mineral sorption sites for SOC, so mineral type, charge, and reactive surface area become important controls on SOM stabilization. At depth, decomposition can also be limited by the physical disconnection between microbes and SOC caused by spatial heterogeneity (Gleixner, 2013; Heinze et al., 2018).

Compared to the research on surface litter decomposition, few studies have examined how decomposition of plant litter changes with depth in situ (e.g., Bird and Torn, 2006; Gill and Burke, 2002; Solly et al., 2015), and even fewer have examined decomposition throughout the top meter of the soil profile (e.g., Gill and Burke, 2002; Preusser et al., 2017; Sanaullah et al., 2011). Results from these studies have shown that in situ decomposition rates are initially similar across depths. However, Hicks Pries et al. (2017a) recently showed that decomposition, particularly of the <2 mm soil fraction, slowed in the A horizon relative to the O horizon between the fifth and tenth years of decay, likely as a result of organo-mineral associations. Similarly, a litter bag study of root decomposition found that mass loss rates declined linearly from 10 to 100 cm (Gill and Burke, 2002).

As with studies tracking the loss of fresh litter inputs in situ, results from incubations that measured how the respiration of SOC changes with depth have been equivocal. When carbon losses are normalized by SOC content, incubations have shown similar decomposition rates across depths (Salomé

et al., 2010), faster decomposition rates in deeper soils (Wordell-Dietrich et al., 2017), and slower decomposition rates in deeper soils (Gabriel and Kellman, 2014; Gillabel et al., 2010). In one incubation study, sieving increased respiration rates from subsoils but not from surface soils, implying SOC at depth was either protected in aggregates or physically separated from microbes (Salomé et al., 2010). Other incubation studies have shown positive priming effects with the addition of glucose (Karhu et al., 2016), cellulose (Fontaine et al., 2007), or organic acids (Heitkötter et al., 2017) in deeper soils, indicating that decomposition at depth is energy-limited.

The processes behind declines in SOC turnover rates with depth have not been explicitly included in most SOC modeling studies. While past modeling studies have included a decline in SOC turnover rate as a function of depth, this was typically done using empirical parameterization rather than a process-based approach (e.g., Jenkinson and Coleman, 2008; Koven et al., 2013). Koven et al. (2013) speculated that this pattern could be due to oxygen availability or priming effects but did not explicitly simulate these processes. Recent developments in explicitly modeling microbial decomposition and organo-mineral interactions (e.g., Sulman et al., 2014) now allow us to explicitly simulate interactions between C inputs and microbial growth. We can use these tools to investigate the extent to which stimulation of microbial activity by fresh C inputs near the surface and mineral stabilization of SOC at depth can explain observed declines in SOC turnover with depth. By evaluating these new models in the context of observations, we can move toward placing biogeochemical modeling of subsoils on a firmer mechanistic foundation.

Here, we incubated $^{13}$C-labeled roots in situ at three depths (15, 55, and 95 cm) of a coniferous forest Alfisol over 2.5 years. We aimed to understand how the decomposition process changes with soil depth including C mineralization, biological assimilation by microbes, and transformation of litter C into SOC. Our specific objectives were to 1) quantify differences in total retention and transformations of root litter into fine particulate and mineral-associated organic matter across depths; 2) explore whether patterns in the soil profile explain root decomposition differences and how root decomposition differences may explain observed SOC patterns with depth; 3) investigate how the abundance of microbial groups and their use of the root litter differed with depth using $^{13}$C-specific phospholipid fatty acid analysis; 4) use an SOC decomposition model with explicit representation of microbial decomposition and SOC-mineral interactions (Sulman et al., 2014) to test whether microbial responses to root exudates could explain decomposition differences across depths.

## 2. Methods

### 2.1. Study site

The University of California Blodgett Experimental Forest is located in the foothills of the Sierra Nevada near Georgetown, CA at 120°39′40″W;

38°54′43″N at 1370 m above sea level and below the permanent winter snowline. Mean annual precipitation is 1774 mm, with most of it occurring from November through April. Mean annual temperature is about 12.5 °C (Bird and Torn, 2006). The decomposition experiment was in a thinned 80-year-old stand of mixed conifers including ponderosa pine (*Pinus* ponderosa), sugar pine (*Pinus lambertiana*), incense cedar (*Calodefrus decurrens*), white fir (*Abies concolor*), and douglas fir (*Pseudotsuga menziesii*). The soils are Holland series: fine-loamy, mixed, superactive, mesic Ultic Haploxeralfs of granitic origin with thick, >5 cm O horizons (Rasmussen et al., 2005). Soil temperature and volumetric water content were measured continuously at multiple depths in the top meter in nearby (within 100 m) control plots of a soil warming experiment as described in Hicks Pries et al. (2017b).

### 2.2. Soil characterization

Three soil pits within 120 m of each other were dug to a depth of 100 cm in August 2013. Coarse (>2 mm) and fine (<2 mm) roots were sampled from 0 to 10, 10–20, 20–30, 30–50, 50–80, and 80–100 cm depths within 25 × 25 cm quadrats while the soil pits were dug. We characterized the profiles according to procedures outlined in the NRCS Soil Manual (2017), delineating the depth of each genetic horizon. Bulk density was sampled in the center of each soil horizon (5–6 horizons per pit) using a small handheld hammer corer (5.35 cm in diameter by 10 cm long; Table S1). For all other soil analyses, we collected 10 cm long increments of soil that were 4 cm wide by 4 cm into the pit face from 0 to 100 cm for a total of 10 samples per pit. Soil samples were stored at 4 °C in plastic bags. Within two days, we processed the soil samples in the lab. Bulk density samples were sorted to remove roots and rocks, weighed, and a 10–15 g subsample was dried at 105 °C until it maintained a constant weight to determine moisture content. The soil sampled in 10 cm increments similarly had roots and rocks removed and was then dried at 50 °C for 4 days. A subsample of the dried soil was ground with stainless steel balls in stainless steel canisters on a roller mill for 48 h and if necessary, on a Spex mill, and then analyzed by Elemental Analyzer-Isotope Ratio Mass Spectrometer (EA-IRMS; IsoPrime 100 IRMS in line with a Vario micro cube EA, Isoprime, United Kingdom) for %C, %N, $\delta^{13}C$, and $\delta^{15}N$. For all depths and analyses, there are three reps, one per soil pit.

Microbial biomass C (MBC) was measured using a modified fumigation-extraction procedure (Joergensen and Mueller, 1996; Vance et al., 1987). In brief, duplicate 20 g field-moist samples were either extracted immediately with 80 ml of 0.05 M $K_2SO_4$ for an hour and then filtered through a Whatman #1 filter or extracted similarly after fumigation in a chloroformatmosphere for five days to ensure chloroform reached all soil pores. Extracts were diluted and run for TC on a Shimadzu TOC-V Analyzer (Shimadzu North America, Columbia, MD). MBC was calculated as the difference between TC in fumigated and non-fumigated samples, divided by a correction factor of 0.45 (Beck et al., 1997). Soils were sampled for MBC in June 2014, 2015, and 2016, as well as in December 2014 from 10 to 20, 50 to 60, and 80 to 90 cm.

Benzene polycarboxylic acids (BPCA) were used as a proxy for pyrogenic C in the soil samples and were measured according to Wiedemeier et al. (2016, 2013). The BCPA yields were directly reported as BPCA-C (%SOC), without the use of a conversion factor. Performance and high reproducibility were checked by measuring samples in triplicates and simultaneously running external standards (Wiedemeier et al., 2016).

### 2.3. Root decomposition

To grow $^{13}C$-labeled roots, in 2013, *Avena* fatua seeds were sown in a 50:50 mixture of vermiculite and sand and grown in a greenhouse within an airtight chamber. A Li-Cor 840 (LiCor, Nebraska) and datalogger (CR800, Campbell Scientific) monitored the air inside the chamber and opened a solenoid valve to let in $CO_2$ when concentrations dropped below 390 ppm. About every 4 days the source of $CO_2$ was switched between tanks of unlabeled $CO_2$ and 10 atom% $^{13}CO_2$ (Cambridge Isotope Laboratories, Inc., Massachusetts, USA). The plants were watered on an 'as needed' basis. We harvested the *Avena* after it went to seed by cutting off the stems and then shaking the roots loose from the potting mixture and rinsing the roots in water. The *Avena* material was then dried for a week at 40 °C. Three subsamples of the roots were ground and analyzed for %C and $^{13}C$ using a Thermo Delta V Plus isotope ratio mass spectrometer interfaced to a Costech ECS 4010 CHNSO analyzer (EA-IRMS) at the Center for Isotope Geochemistry at Lawrence Berkeley National Laboratory. The %C and $^{13}C$ were 46.3% and 4255‰, respectively (Castanha et al., 2018).

We added 0.5 g of dried *Avena* fine root (<2 mm diameter) at each of three depths (15, 55, and 95 cm) to three walls of each soil pit ($n = 3$) in November 2013, so that each pit would have three sets of roots, one for each of the collection times. The depths corresponded to the AB, Bt, and BC genetic horizons, respectively. This amount of C was equivalent to 2%, 8%, and 11% of the native SOC pool at 15, 55, and 95 cm, respectively. *Avena fatua* is an annual grass; its roots were used as a common substrate so that its decomposition could be compared across studies (e.g., Castanha et al., 2018). These roots (C:N = 39) were likely more decomposable than the coniferous roots native to the site (Silver and Miya, 2001). At each depth, the roots were added to a 10.2 cm diameter circular area. Each area had twenty, 4 cm deep (into the pit wall) holes that were created by a 2.5 mm diameter metal stake in which we inserted 4 cm long bunches of fine roots (≈0.025 mg). We inserted the roots this way to minimize soil structure disturbance. We marked where the roots were placed using tent stakes below the insertion area and placed mesh (fiberglass window screen) over each side of the pit before filling the pit back in. The mesh allowed us to find the sides of the pits when we had to dig them out again to collect the incubated roots.

The first collection of the root litter took place in June 2014 (6 months) and subsequent collections occurred in November 2014 (12 months) and June

2016 (30 months). To collect the root litter and associated soil, we used a capped and sharpened PVC collar (10 cm in diameter by 10 cm deep) that we hammered into the side of the pit around where the roots had been inserted. We used another PVC sampler to collect control soil from the same depth and side of the pit about 20 cm away from the root sample. After collection, the pits were refilled. The samples were stored in plastic bags at 4 °C. In the laboratory, samples were sieved through a 2-mm mesh into coarse particulate (CPOM, > 2 mm, included identifiable root litter pieces) and bulk soil (<2 mm) fractions, weighed, freeze-dried, and re-weighed to determine moisture content. Dried subsamples were ground and analyzed for %C, %N, and $\delta^{13}C$ using the aforementioned EA-IRMS.

The bulk soil fraction was further separated by density into free light (fLF) occluded light (oLF), and dense fractions (DF) using a 1.7 g $ml^{-1}$ sodium polytungstate solution and methods refined in our lab (Bird and Torn, 2006; Swanston et al., 2005). We added 50 ml of 1.7 g $ml^{-1}$ of low C/N sodium polytungstate solution ($SPT_0$, TC-Tungsten Compounds Inc., Grub am Forst, Germany) to 20 g of air-dried soil in a conical based polycarbonatecentrifuge bottle. The bottle was gently inverted several times to ensure that all soil was in contact with the SPT solution. Any remaining soil particles were rinsed from lids and rims of centrifuge bottles and the samples were left to equilibrate on the bench top for 1hr to ensure maximum separation between light and mineral associated fractions before being centrifuged in a swinging bucket rotor for 1 h at 3500 rpm (4710 × g) and 25 °C. The fLF (<1.7 g $ml^{-1}$) was vacuum aspirated from the centrifuge bottle, filtered through a 0.8 µm polycarbonate filter (Nucleopore Track-Etch, Whatman), and rinsed with Nanopure reagent grade water (18.2 MΩ-cm) until the filtrate was the density of water. Aggregates were physically disrupted by mixing the remaining sample in SPT solution using a benchtop mixer (G3U05R, Lightnin) at 75% power for 1 min followed by sonication (Branson 450) in an ice bath at maximum output and 70% pulse for 1.5 min for a total energy input of 100 J $ml^{-1}$. The samples were equilibrated for one hour on the bench top and subsequently centrifuged for 1 h at 3500 rpm (4710 × g), allowed to settle overnight followed by vacuum aspiration of the floating material, the oLF, which was then filtered and rinsed following the same procedure as for the fLF. The remaining sample, the DF, was rinsed of residual SPT with Nanopure water until the supernatant was the density of water. A flocculant consisting of 30 ml of 1 M $CaCl_2$ in 3 ml of 1 M HCl was added to samples prior to rinsing to prevent dissolution of metal oxide minerals and ensure complete recovery of sample material. All fractions were dried at 105 °C, weighed, ground, and analyzed for %C, %N, and $\delta^{13}C$ by EA-IRMS. Average recoveries were 101% for mass and 88% for C.

The amount of root litter-derived C recovered in each fraction was calculated by multiplying the fraction of litter-derived C by the total amount of C in that fraction. The proportion of litter-derived C in each fraction was calculated using a simple mixing model:

$$IAR = fsoil * IC + froot * Iroot$$

$$1 = fsoil + froot$$

where $I$ is the isotopic content ($\delta^{13}C$), subscript $AR$ denotes the value of the soil, fraction, or phospholipid fatty acid (PLFA) that had root litter added to it, $C$ denotes the control value from the corresponding pit, depth, timepoint (except for CPOM, in which we only used timepoint 3 of the controls), and PLFA (where applicable), and *root* denotes the value of the labeled root litter. $f_{soil}$ is the proportion of C derived from native soil and $f_{root}$ is the proportion of C derived from the labeled litter. The percent of litter-derived C remaining was calculated as the amount of recovered C divided by the total amount added to the soil at the beginning of the experiment multiplied by 100.

### 2.4. Phospholipid fatty acid analysis

In order to identify soil microbial communities and their assimilation of the labeled root substrate by depth, a PLFA extraction was performed on freeze-dried soils using previously described procedures (Bird et al., 2011; White and Ringelberg, 1998). Approximately 10 g of soil was analyzed for the 15 and 55 cm depths, and 12 g for 95 cm in order to compensate for lower microbial biomass at depth (Fierer et al., 2003). Recovery from samples was determined using di-19:0 PC (1, 2-Dinonadecanoylsn-Glycero-3-Phosphocoline, Avanti Polar Lipids, Alabaster, AL, USA), which was added to the soils before the extraction. Additionally, a 10:0 fatty acid methyl ester standard (FAME; ethyl decanoate, Sigma-Aldrich, Inc., St. Louis, MO, USA) was added to samples prior to gas chromatography. The FAMEs were analyzed on a Hewlett Packard (Agilent) 5890 Series II Gas Chromatograph (GC) with a 30 m × 0.32 mm x 1.0 mm ZB-5 column (Phenomenex, Inc., Torrance, CA, USA) connected via a Europa ORCHID on-line combustion interfaced to an IsoPrime 100 Isotope Ratio Mass Spectrometer (IRMS, IsoPrime, Cheadle, UK). Bacterial fatty acid standards were used to identify peaks (MIDI, Newark, DE).

PLFA biomarkers were used to quantify the relative abundances of different microbial groups. Thirteen PLFA biomarkers were assigned to six categories: Gram-positive bacteria (15:0i, 15:0a, 17:0i, 17:0a), Gram-negative bacteria (16:1u7, 18:1u7), fungi (18:2u6,9, 18:1u9), actinobacteria (16:010Me, 18:010Me), protozoa (20:4u6,9), and cyclopropyl bacterial (17:0cyc, 19:0cyc) (Zelles, 1999; Zogg et al., 1997). Unassigned PLFAs (14:0, 14:0i, 15:0, 15:1i, 16:0, 16:0 12Me, 16:0i, 16:1 2OH, 16:1i, 16:1w5c, 16:1w9c, 17:0, 17:0 10Me, 17:1w8c, 18:0, 18:1w5c, 18:1w7c 11Me, 20:0, 20:1w9c, i17:1) were included in total PLFA yields and community analyses (Bird et al., 2011). The IRMS was used to determine the $\delta^{13}C$ so the proportion of PLFA-C incorporating the $^{13}C$-labeled root substrate could be identified using the mixing model described above. The preference for added root or native soil C was quantified by subtracting the mole percent of native soil-derived C from the mole percent of labeled root-derived C in each PLFA.

## 2.5. CORPSE model

The Carbon Organisms Rhizosphere and Protection in the Soil Environment (CORPSE) model simulates soil organic matter formation and decomposition with a focus on microbial and mineral interactions (Fig. 1; Sulman et al., 2014). See the Supplemental Information for full model equations and parameters and the code used to run the model. Organic substrates are divided into three chemically-defined classes representing rapidly-decomposing compounds (such as sugars and cellulose), slowly-decomposing compounds (such as lignin), and microbial necromass. Decomposition of these substrates is controlled by a dynamic microbial biomass pool. Rapidly-decomposing compounds have high maximum decomposition rates and microbial carbon use efficiencies, and as a result they stimulate microbial growth, allowing the model to simulate acceleration of decomposition through inputs of fresh organic matter and root exudates (priming effects). Organic substrates exist in either unprotected or protected forms, with protected organic matter temporarily inaccessible to microbial decomposition. Organic matter is transferred between unprotected and protected pools at fixed rates, with microbial necromass having a higher protection rate than other substrates. The model structure allows organic matter to be divided into isotopically labeled and unlabeled fractions to facilitate comparison with isotope tracking measurements but does not simulate any isotopic fractionation via biochemical processes.

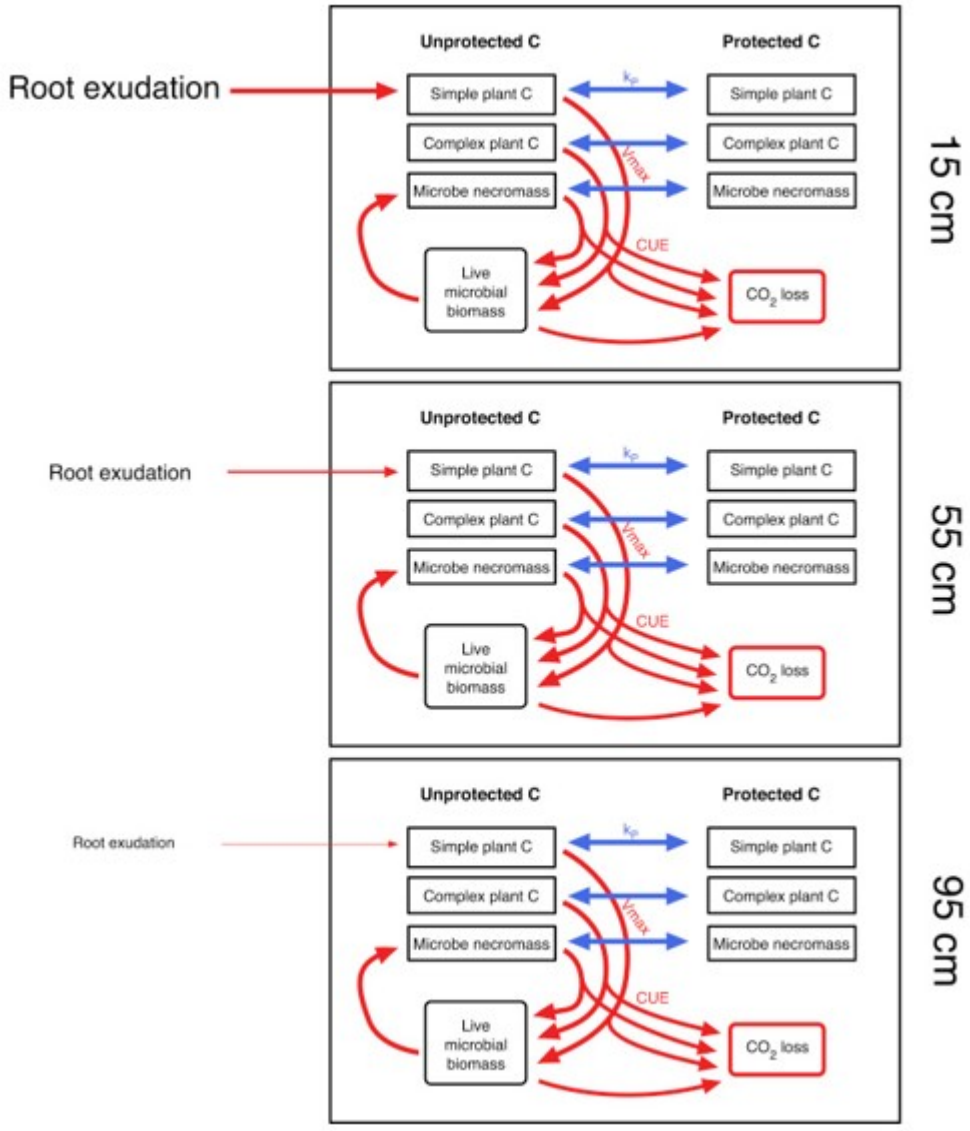


Fig. 1. Diagram of the CORPSE model applied to different soil depths. Model structure and initial root carbon were identical at each depth, while root exudation rates differed by depth. Red arrows show decomposition-related carbon flows and blue arrows show protection-related carbon flows.

We simulated decomposition of isotope-labeled root litter by initializing the model with 0.5 mg of root mass, which was assumed to contain 25% rapidly-decomposing compounds and 75% slowly-decomposing compounds in line with previous CORPSE simulations (e.g., Sulman et al., 2017). We drove the model for the 15, 55, and 95 cm depths by interpolating measured profiles of soil temperature and moisture to the appropriate depths. In addition, each depth received root exudate inputs calculated based on the observed profile of living fine roots. Root exudation rate was calculated based on measured fine root (<2 mm) biomass at each depth, following estimates of exudation per fine root biomass from Phillips et al. (2011) and assuming that exudation rates were relatively higher nearer the surface to account for other sources

of fresh carbon such as leaching from the litter layer. The resulting input rates per unit root biomass were 26.2 mg C g root$^{-1}$ year$^{-1}$ at 15 cm depth and 6.5 mg C g root$^{-1}$ year$^{-1}$ at 55 and 95 cm depths, and input rates per unit soil volume were 0.13 mg C cm$^{-3}$ year$^{-1}$ at 15 cm depth, 0.0094 mg C cm$^{-3}$ year$^{-1}$ at 55 cm depth, and 0.0082 mg C cm$^{-3}$ year$^{-1}$ at 95 cm depth. To capture the range of potential decomposition environments due to the high spatial heterogeneity at depth, we also ran an additional simulation at 95 cm depth without any root exudate inputs.

### 2.6. Statistical analyses

We analyzed the measured data using linear models in R (R Development Core Team, 2017) with the continuous variables (depth and time) as the main effects and a depth by time interaction. For analyses of root recovery in fractions, fraction—bulk and particulate or free light, occluded light, and dense—was an additional fixed effect. For PLFA analyses, PLFA or biomarker and treatment (control or labeled) were additional fixed effects. We used Akaike's Information Criteria (AIC)-based model selection to determine whether variance structures or a random effect, in this case soil pit, improved the models following Zuur et al. (2009). We also used stepwise model reduction and AIC to determine which fixed effects and interactions were significant in the models. We tested all 2-way and 3-way interactions. When interactions among continuous main effects were significant, we set up multiple comparisons using the lstrends command in the lsmeans package (Lenth, 2016). For each fraction (where applicable), we tested depth slopes with time set at 6, 12, and 30 months and time slopes with depth set at 15, 55, and 95 cm; we used the multivariate *t* distribution to test for significance at $\alpha < 0.05$ taking into account the number of multiple comparisons. When only categorical main effects were significant, we performed contrasts with a Tukey adjustment in lsmeans with the continuous main effects held at their mean values. We also fit an exponential decay model to the total recovery data using the nls package in R and chose the best model based on AIC (Tables S1 and S2).

## 3. Results

### 3.1. Soil characterization

We characterized how SOC, root biomass, microbial biomass, and climate (temperature and moisture) changed with depth. These soils stored $16.6 \pm 1.7$ kg C m$^{-2}$ in the top meter of mineral soil, with 45% of this SOC stored below 20 cm. Carbon concentrations decreased from 8.3% in the top 10 cm to an average of 0.37% below 60 cm (Fig. 2a). Nitrogen concentrations also decreased, from 0.3% at the surface to 0.01% below 60 cm. The C:N ratio decreased from 28 in the top 10 cm to 23.6 at 60–70 cm before increasing to 34 at 90–100 cm (Fig. 2b). $\delta^{13}$C became enriched from 0-10 cm to around 60–70 cm before it became more depleted towards 90–100 cm (Fig. 2c). Pyrogenic C was most concentrated at 15 cm and had similar, low concentrations at 55 and 95 cm (Fig. 2d). Fine root (<2 mm) density declined

steeply in the top 40 cm while coarse root (>2 mm) density peaked around 40 cm (Fig. 2e). The proportion of SOC in the three density fractions differed significantly ($p < 0.0001$). About half of SOC was in the dense fraction and 23–36% in the free light fraction (Fig. 2f); however, the distribution of SOC among the fractions did not differ significantly by depth (depth × fraction interaction, $p = 0.11$). Microbial biomass declined more linearly with soil depth than did SOC (Fig. 2g). The ratio of microbial biomass C to SOC was ≈10 mg $g^{-1}$ at both 15 and 95 cm but was 22 mg $g^{-1}$ at 55 cm. Soil bulk density increased with depth while pH generally decreased from 6.2 at 5 cm to 5.6 at 75 cm before increasing to 6.5 at 95 cm (Tables S1 and S2). Soil temperature and volumetric water content averaged 11°C and 26% over the 2.5-year experiment, respectively, and the averages did not differ among depths (Fig. 2h and i). However, surface soils experienced a more temporally variable climate than deeper soils (Fig. S1).

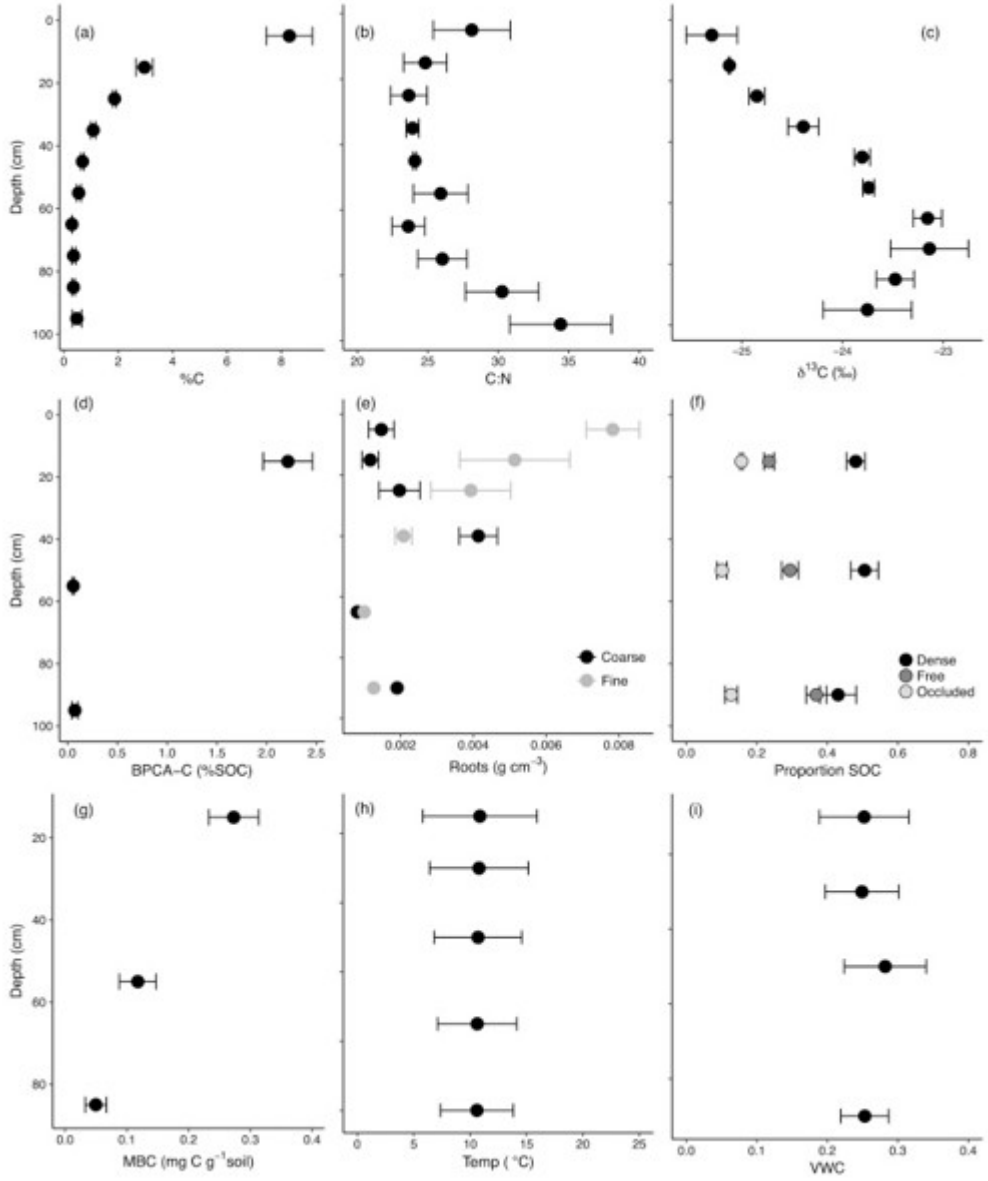


Fig. 2. Soil profiles of mean ± SE (n = 3 soil pits) percent carbon (a), C:N ratio (b), $\delta^{13}C$ (c), BPCA as a percent of total SOC (d), root density for coarse and fine roots (e), the proportion of SOC found in dense, free light, and occluded light fractions (f). The bottom row contains mean ± SE (n = 3 soil pits) microbial biomass (g; averaged over four timepoints: June and December 2014, June 2015, and June 2016), and mean ± SD (averaged over time to show temporal variability) soil temperature (h) and soil volumetric water content (i) over the course of the experiment (November 2013 through June 2016) from n = 3 control plots of an adjacent experiment.

## 3.2. Root decomposition

Loss of root litter C during the first 6 months was similar across all depths with 62% of applied root C remaining (Fig. 3). However, after 30 months, root C loss was significantly faster at 15 cm than at 55 cm and significantly faster at 55 cm than at 95 cm with 25, 40, and 62% of applied root C remaining, respectively. In the regression model, these differences in retention with

depth resulted in a significant depth × time interaction ($p = 0.017$, $f = 6.7$, $df = 1$). Recoveries after 6 and 12 months were similar across depths but differed across depths after 30 months ($p < 0.05$). We also fit an exponential decay model to the data (Fig. S2, Table S3). The best fit model, based on AIC, was a double exponential decay model with the parameter controlling the decay rate of the slow pool controlled by depth (Table S4). With this model, the estimated turnover times were about 0.3 years for the fast-decaying pool and 3, 6–9, and 7–10,000 years for the slow-decaying pool at 15, 55, and 95 cm, respectively. The wide range in values at 95 cm was due to fitting the model with and without the outlier from the 30-month sampling, which showed zero mass loss after 12 months, and reflected the spatial heterogeneity of soils at depth (Table S3).

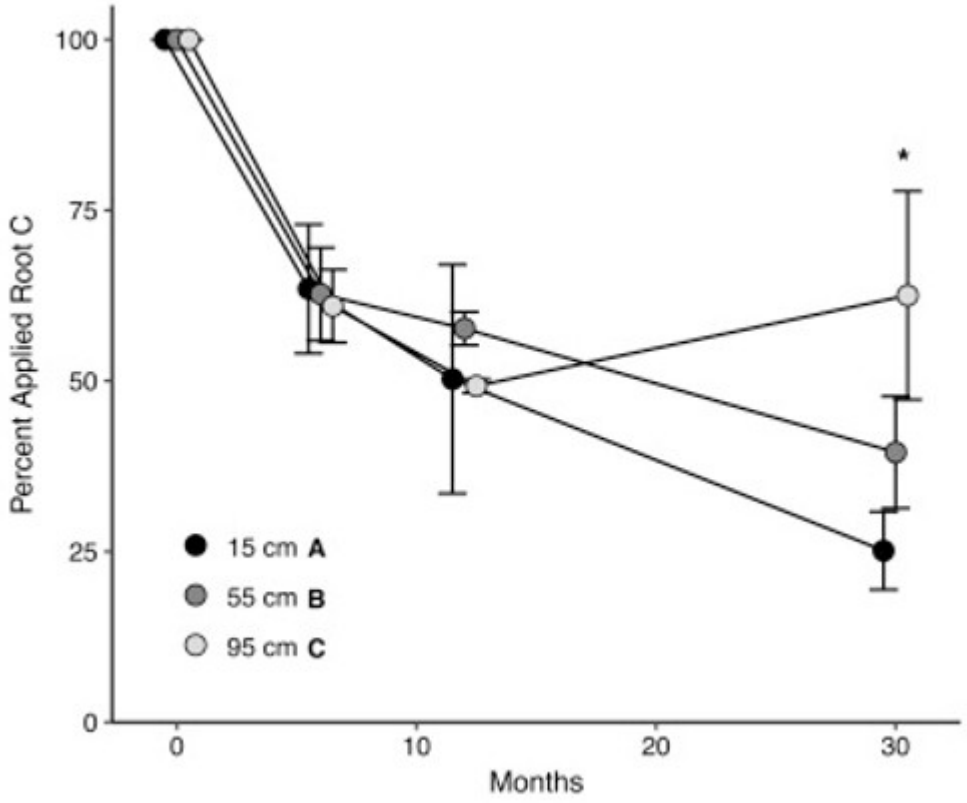


Fig. 3. The percent of total applied root C recovered at 15, 55, and 95 cm depths after 6, 12, and 30 months of in situ incubation (mean ± SE, $n = 3$). The total amount of applied root C recovered decreased significantly with year ($p = 0.0017$). There was also a significant depth × month interaction ($p = 0.017$) because recoveries after 6 and 12 months were similar across depths but differed across depths after 30 months ($\alpha = 0.05$, indicated by asterisk). Furthermore, the slopes of the time trend differed significantly among the three depths ($\alpha = 0.05$, represented by letters not shared).

At each sampling point, the amount of applied root C recovered in the bulk soil fraction (<2 mm) was significantly smaller than the amount recovered in the coarse particulate fraction (i.e., as identifiable root pieces, $p = 0.009$; Fig. 4). The loss of the coarse particulate fraction drove the decrease in the amount of total root C recovered over time at 15 and 55 cm (time × fraction

interaction, $p = 0.08$), but the coarse fraction did not decrease over time at 95 cm (time × depth interaction, $p = 0.02$). As a result, there was more root C recovered in the coarse particulate fraction at 95 cm than at 15 or 55 cm, but similar amounts of root C recovered in the bulk fraction at 30 months (depth × fraction interaction, $p = 0.009$). Within the bulk fraction, the percent of root C recovered among the three density fractions did not differ by depth ($p = 0.58$) or time (6 and 30 months only, $p = 0.97$) but did differ significantly by fraction ($p < 0.0001$; Fig. 5). Among the density fractions, none of the two-way interactions with time, depth, and fraction were significant ($p > 0.25$).

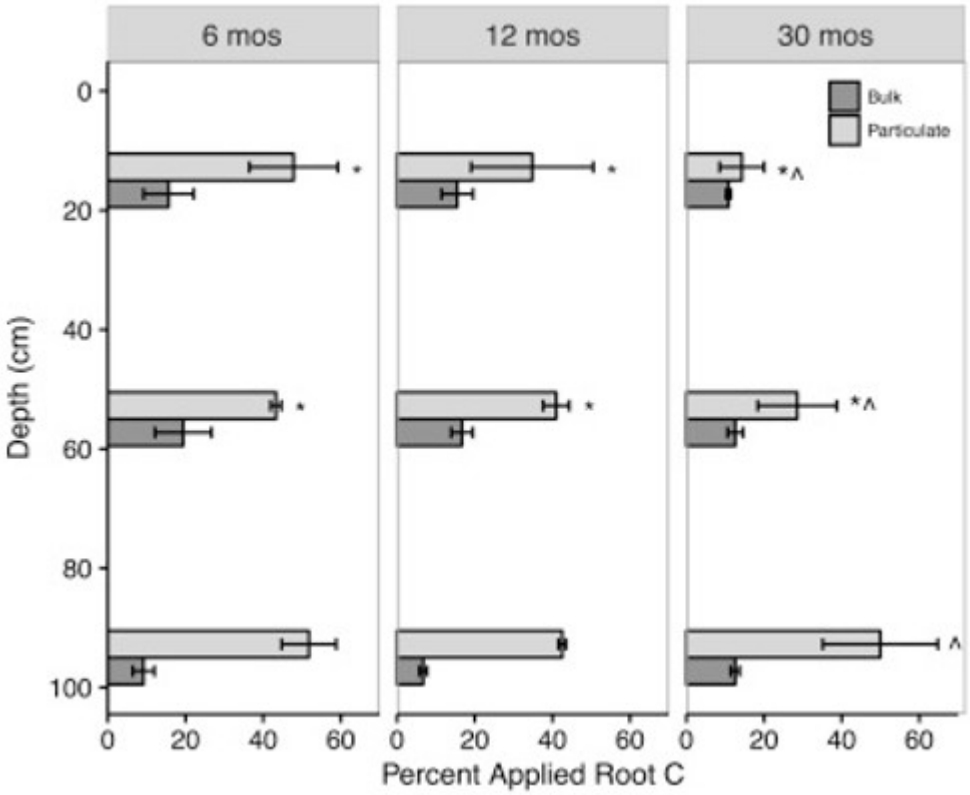


Fig. 4. The percent of applied root C recovered in bulk (<2 mm) and coarse particulate (>2 mm) size fractions over 6, 12, and 30 months of incubation within three depths of the soil profile (mean ± SE, $n = 3$). Asterisks indicate at which depths and for which fraction the declining recovery with time trend was significant and upward carets indicate at which time and for which fraction the depth trend was significant ($\alpha = 0.05$).

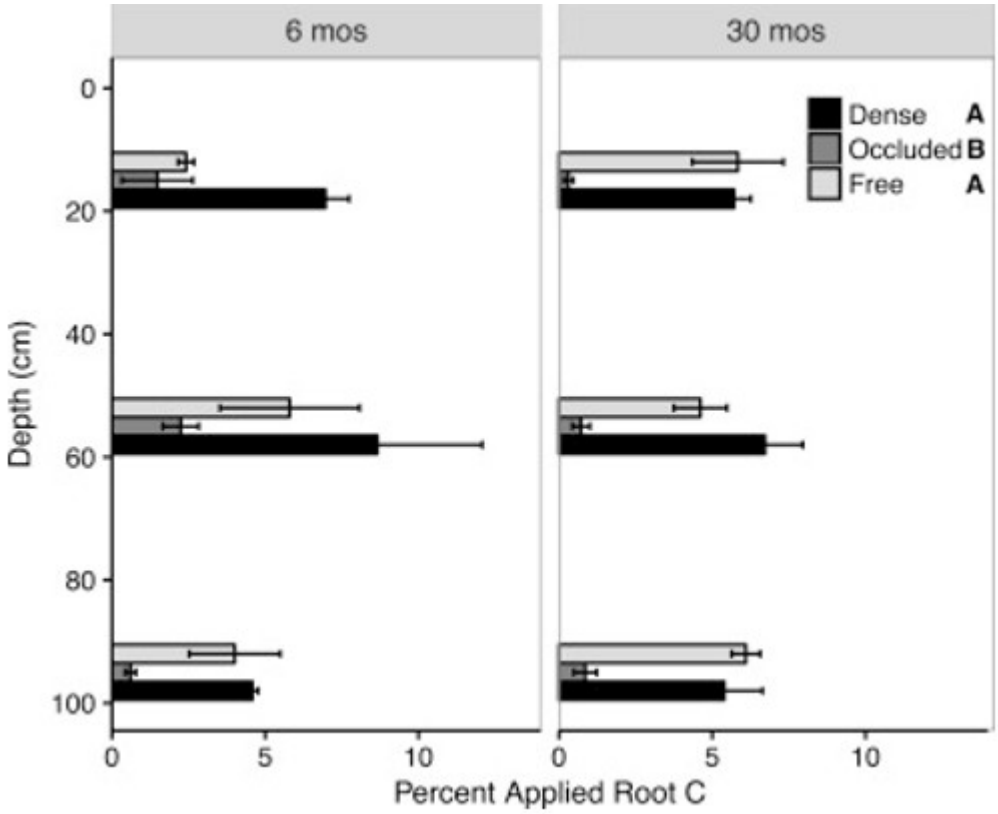


Fig. 5. The percent of applied root C recovered in three density fractions of the bulk soil—dense (>1.7 mg/L), occluded light (<1.7 mg/L), and free light (<1.7 mg/L)—after 6 and 30 months within the soil profile (mean ± SE, n = 3). The amount of root recovered was significantly greater in the dense and free light fractions than in the occluded fraction ($p < 0.05$) as indicated by letters not shared.

### 3.3. Phospholipid fatty acids

There were no significant differences in the relative abundances of PLFA's between the control soils and soils to which labeled roots had been added ($p = 0.63$, $f = 0.23$, $df = 1$). Looking at just the control soil, there were significant changes in certain biomarker abundances with depth (depth × biomarker interaction, $p = 0.0001$; Fig. 6a). The abundances of the fungal biomarker, 18:1w9c, and the Gram-negative biomarker, 18:1w7c, both decreased significantly with depth. The two actinomycetes biomarkers, 16:0 10 Me and 18:0 10Me, both increased significantly with depth. We investigated whether the different microbial groups preferred the native soil C or added root C (Fig. 6b). The actinomycetes biomarkers showed a preference for the native soil C, while the fungal and Gram-negative biomarkers showed a preference for the added root C. The Gram-positive biomarkers did not show a preference. In general, the microbes whose relative abundances increased with depth showed a preference for native SOC, while the microbes whose relative abundances decreased with depth showed a preference for added root C.

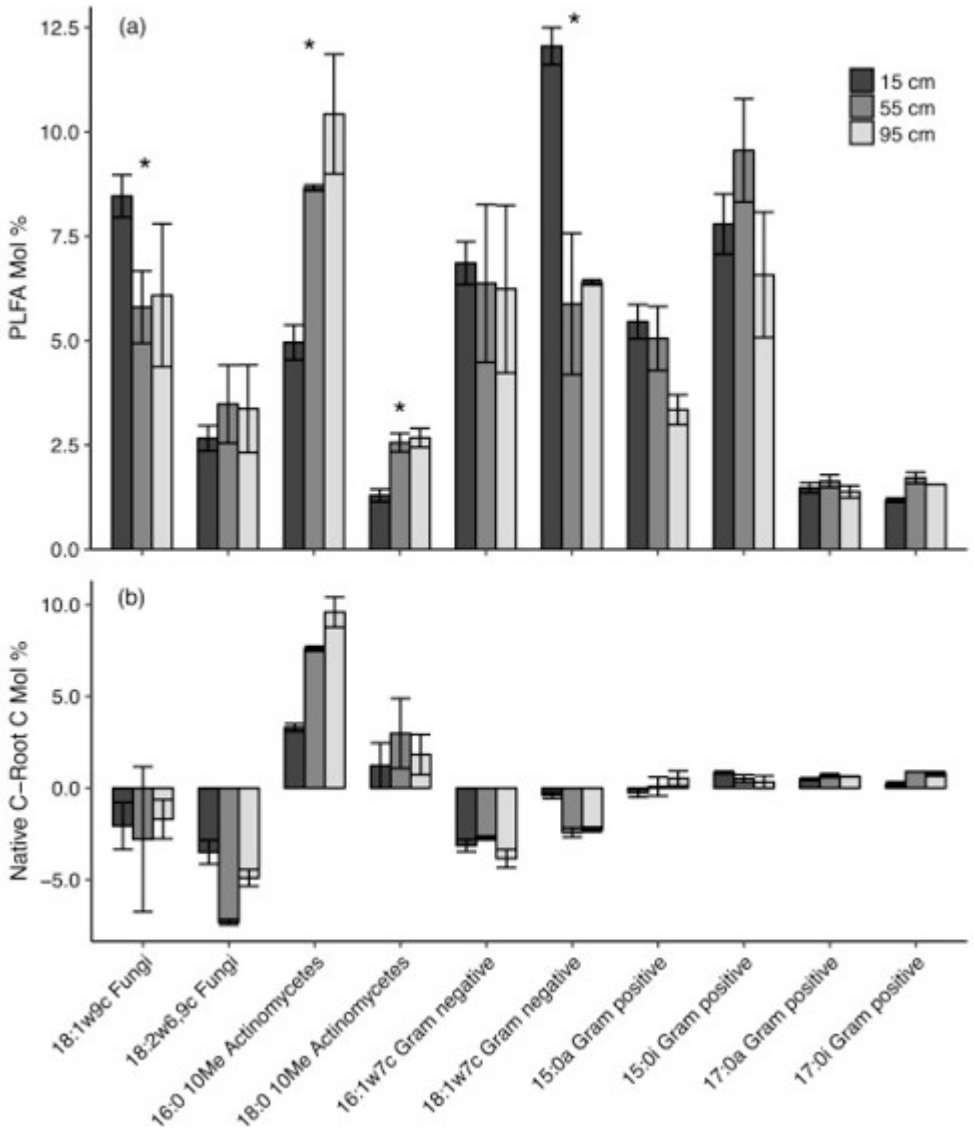


Fig. 6. The relative abundances of a subset of phospholipid fatty acids (PLFAs) associated with microbial biomarkers found at 15, 55, and 95 cm within the control samples (a). The asterisks indicate which PLFA's abundances significantly changed with depth ($p < 0.08$ for contrasts, depth × biomarker interaction, $p = 0.0001$). The relative amounts of C derived from native soil and C derived from the labeled roots after 6 months in each of the biomarker PLFA's (b). A positive value indicates native C was preferred and negative values indicate the labeled root C was preferred while values around zero indicate no preference.

## 3.4. CORPSE model simulations

Results from the CORPSE model simulations agreed with observations showing that initial rates of root C loss were similar across depths in the first year of decomposition but diverged afterwards (Fig. 7a). At 30 months, decomposition was projected to be fastest at 15 cm and slowest at 95 cm, where root exudate inputs were lower. Similar patterns across time and depth were projected in the amount of root C remaining in the unprotected pool, which is similar to the coarse particulate plus the free light fraction

measured in the experiment (Fig. 7b). In contrast, the amount of root C remaining in the protected pool, similar to the dense fraction, reached an asymptote around 5% between 6 and 10 months and was similar across depths (Fig. 7c). The model results matched the observed patterns of remaining root C in the total, unprotected (coarse and fine particulate), and protected (dense, mineral-associated) fractions, with two exceptions. First, differences in total root C remaining among depths at 30 months were greater in the experiment than were predicted by the model, and second, the initial decomposition rate and subsequent loss of C from the unprotected pool and gain of C in the protected pool were faster in the experiment. We also compared turnover times estimated from CORPSE simulations with estimates from the double exponential decay model fitted to experimental observations (Tables S1 and S3). Initial turnover times estimated for the first 6 months by CORPSE were 1.3–1.4 years versus 0.28–0.32 years for the fast-decaying pool of the exponential decay model (Tables S3 and S5 and Fig. S3). Longer-term turnover times were more similar, with 3.6 and 3.8 years at 15 cm and 8.6 and 9.1 years at 55 cm, estimated by CORPSE and the exponential decay model, respectively. Both the CORPSE and exponential decay model estimated wide ranges in longer-term turnover times at 95 cm: ranging from 10.8 to 82.8 years, with and without exudates in CORPSE, and from 7 to 10,000 years, depending on the inclusion of the 30-month outlier from the data.

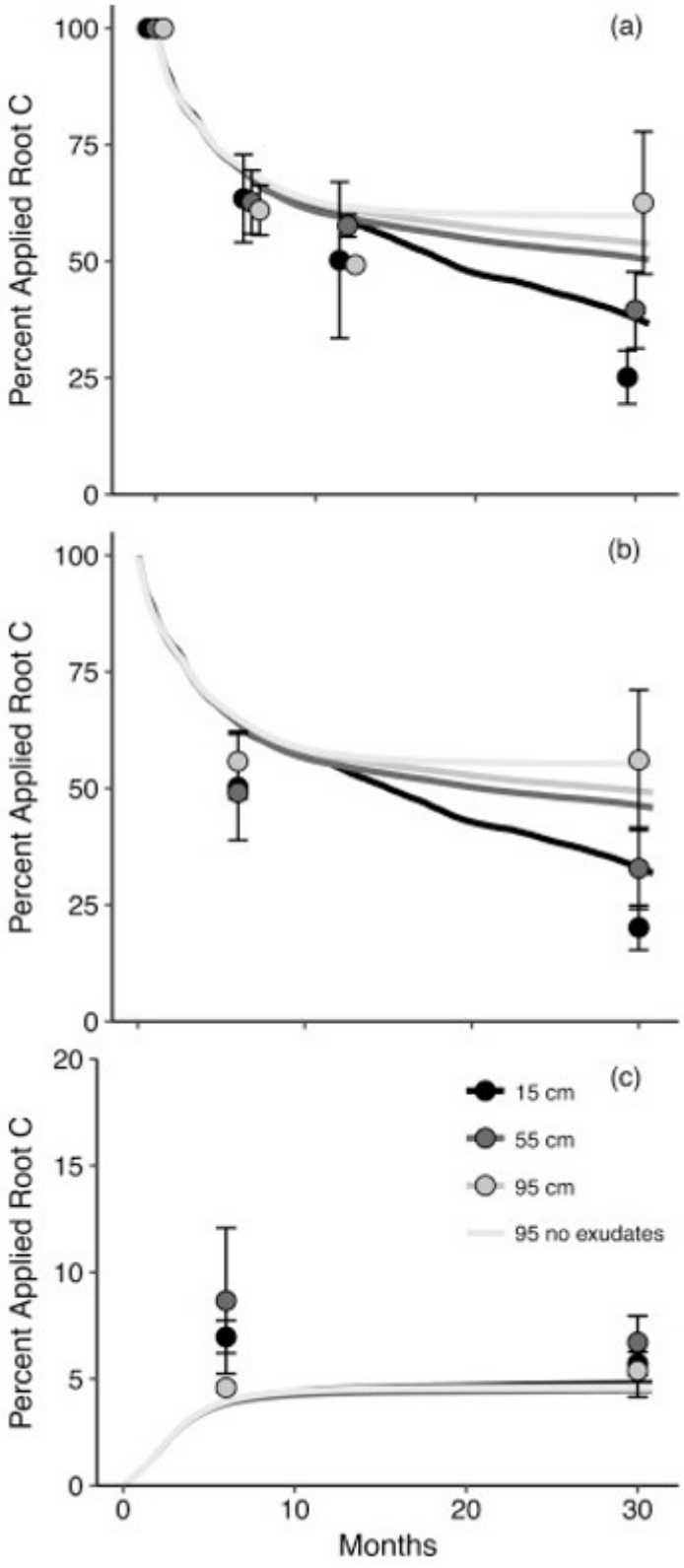
(a)
(b)
(c)
Percent Applied Root C
Months
15 cm
55 cm
95 cm
95 no exudates
0
25
50
75
100
5
10
15
20
30

Fig. 7. Results of the CORPSE model (lines) and the experimental observations (mean ± SE, circles) for total root C remaining (a), root C remaining in unprotected pools (b), and root C remaining in protected pools (c). To match the pool structure of the CORPSE model, we assigned the coarse particulate plus the free light fraction from the experiment to the unprotected pool and the dense, mineral-associated fraction from the experiment to the protected pool. The CORPSE model was run twice at 95 cm—once with root exudates proportional to root biomass at that depth and once with no root exudates to demonstrate the range of conditions at depth due to high spatial heterogeneity.

## 4. Discussion

Other than decreasing SOC concentrations, the biggest changes with depth in the soil profilewere biotic—both microbial and root biomass decreased. In contrast to other soil profiles (Kögel-Knabner et al., 2008; Schrumpf et al., 2013), however, the proportion of SOC that was mineral-associated did not increase with depth. Instead, the proportion of SOC that was mineral-associated (i.e., DF) versus fine particulate (i.e., fLF) remained constant with depth. The average microclimate at all depths was also similar during the experiment, although temperature and moisture extremes were greatest at 15 cm depth. We tested the effect of different soil temperature and moisture regimes among depths with CORPSE, by running the model with the actual soil temperature and moisture at each depth and holding all other parameters constant. This simulation showed only very minor decomposition differences among depths (Fig. S1). Oxygen also did not differ much among depths and was above 16% at all depths (data not shown). Based on the soil profile data we collected, it seems that any differences in root litter decomposition among depths were likely biotically driven.

Mineralization of root litter C was similar across depths over the first 12 months, matching the results of the few previous studies that examined root decomposition across multiple depths in situ (Bird and Torn, 2006; Sanaullah et al., 2011; Solly et al., 2015). However, after 30 months, mineralization differed among depths, as it did after 10 years in the decomposition experiment started by Bird and Torn (Hicks Pries et al., 2017a). Similar initial root mineralization suggests that the microbial potential to decompose the fast-decaying portion of litter inputs is similar at all depths. Over time in situ, however, the litter is fragmented and mineralized more slowly at depth, suggesting that microbial capacity at depth becomes limited as the pool of labile litter C and N are depleted. This was consistent with CORPSE model results, in which initial microbial decay was supported by the labile content of root inputs at all depths but decay rates diverged once this initial pulse of labile C was depleted.

The similar initial root mineralization rates indicate that the conditions for rapid microbial degradation of labile, accessible SOC exists at all depths. Fungi and Gram-negative bacteriapreferentially assimilated the added root-derived C relative to native SOC. Despite greater relative abundances of fungi and Gram-negative bacteria towards the soil surface, the shift in microbial communities with depth did not result in a difference in initial decomposition. Their abundances likely reflected the profile of native SOC substrates, as the addition of root litter did not change microbial

communities at any depth. Microbial biomass per gram SOC was similar at the surface and at 95 cm, and the aforementioned microbial groups that preferred the root litter were present at all depths. Furthermore, the microbes experienced similar microclimates at all depths during the first six months of decomposition with average temperatures of 8.2–8.6 °C and average volumetric water contents of 25–28%.

Slower longer-term root mineralization in deeper soil was not due to root C becoming associated with mineral surfaces. The amount of root-derived C associated with minerals was constant across depths and did not change between 6 and 30 months, remaining at about 5%. In a nearby coniferous forest, 5% of C from root or needle litter was also mineral-associated in the A horizon after 10 years (Hicks Pries et al., 2017a). This potential upper limit on the amount of litter C that could become mineral-associated at this site could indicate C saturation (Castellano et al., 2015; Stewart et al., 2008), but the specific mechanisms leading to C saturation are unclear given the patchy distribution of organic matter on minerals and potential for organo-organo interactions (Vogel et al., 2014). Moreover, it is unlikely that the soil at 55 or 95 cm is C saturated given the paucity of soil C (<0.7%) at those depths. A more plausible explanation for similar amounts of root C becoming mineral-associated is related to the Microbial Efficiency-Matrix Stabilization hypothesis (MEMS; Cotrufo et al., 2015, 2013). MEMS states that the more labile portions of litter become mineral-associated because those portions are most efficiently (i.e., have a higher anabolism:catabolism ratio) converted into microbial residues that can then sorb to minerals. Our experiment's 5% limit on the amount of root litter becoming mineral-associated may depend on characteristics inherent to the litter itself and therefore is the same across depths. The speed at which the root-derived C became mineral-associated in our study—5% within 6 months—supports earlier research hypothesizing that initial decomposition products become sorbed to minerals (Cotrufo et al., 2015; Rumpel et al., 2010; Swanston et al., 2005). The CORPSE model is consistent with the MEMS hypothesis via its assumption that microbial necromass forms the bulk of protected C, and the model successfully captured the observed pattern of 5% of root C becoming “protected” (CORPSE does not explicitly distinguish protection mechanisms between occluded and mineral-associated pools) at all depths.

The main differences in root litter decomposition among depths occurred in the coarse particulate fraction, which was the only size or density fraction that significantly differed in the amount of root-derived C among depths after 30 months. The roots in the coarse particulate fraction, which were still identifiable roots, were likely increasingly resistant to decomposition with depth for several reasons. There was a shift in microbial communities with fewer fungal biomarkers extracted at depth. Saprotrophic fungi preferentially decompose the structural components of roots such as cellulose and lignin (Baldrian, 2017; Dashtban et al., 2010), which may in turn allow bacterial decomposers to access the interior root tissue. The fungal and Gram-

negative biomarkers that preferred the added root substrate were less abundant at depth, which might affect longer term decomposition in ways that did not affect initial decomposition. However, a previous study using $^{13}C$-PLFA found decreasing fungal enrichment in $^{13}C$ from added root litter in an annual grassland as decomposition progressed, implying the fungal role was in initial decomposition (Herman et al., 2012).

The amount of root exudates in our soils likely decreases with depth due to declining fine root biomass. Thus, while differences in microbial communities may result in different root decomposition rates, there is a causality dilemma in that differences in root exudation can drive microbial community differences and may thus be the proximal cause of the observed decomposition differences. Root exudates and associated changes in the rhizosphere soil can increase SOC mineralization rates—by 59% on average according to a recent meta-analysis (Huo et al., 2017). To investigate whether a priming effect could have caused the differences in root decomposition with depth, we compared our observations to simulations using the CORPSE model wherein we decreased root exudate inputs with depth. Priming in the model did not affect initial decomposition rates but did affect longer-term decomposition rates, which matched the observations well in terms of total recovery, recovery in various pools, and both initial and long-term litter C turnover times. In particular, rapid initial mineralization at all depths was supported by labile C present in the root inputs, while long-term mineralization rates diverged once these labile compounds were depleted. This is consistent with the hypothesis that continuing fresh inputs of labile C support faster decomposition in surface soils compared to subsoils. In surface soils, microbes can use the energy provided by exudates to synthesize enzymes needed to decompose the remaining root-derived compounds that have higher energetic barriers to decay (Blagodatskaya and Kuzyakov, 2008). According to this hypothesis, breaking down root-derived OC remaining after the initial phase of decomposition in deeper soils is not energetically favorable given the low availability of labile compounds, so decomposition rates are very slow. Positive priming effects have been induced in incubations of subsoils by adding glucose or organic acids and the priming effects were greater in subsoil than in surface soil, implying labile substrates are more limiting to microbial activity in subsoils (Fontaine et al., 2007; Heitkötter et al., 2017; Tian et al., 2016).

While the CORPSE model does well explaining the trends in our experimental data, it does not fully recreate the magnitude of differences in later stages of root decomposition among depths. There are likely other mechanisms driving faster decomposition at the surface than at depth that were not included in CORPSE model. One mechanism is nitrogen limitation of microbial activity in deeper soils (Heitkötter et al., 2017), which may be likely in our soils where the C:N ratio is greater at depth relative to surface soil. The effects of N on decomposition rates are highly variable, but generally positive for low N environments (Knorr et al., 2005). Nitrogen addition

increases cellulose-degrading enzyme activities (Keeler et al., 2009) and fungal decomposition of low nitrogen, lignin-rich litter (Allison et al., 2009; Jiang et al., 2014). Decomposition at depth can be limited by both nitrogen and labile substrates; a recent incubation experiment found that adding nitrogen to subsoils (30–60 cm) increased the priming response to added glucose by 18% (Tian et al., 2016). Recent work incorporating N cycling into the CORPSE model (Sulman et al., 2017) will allow us to investigate the role of N limitation on subsoil SOC decomposition in future analyses.

Another potential mechanism for slower decomposition of roots in the coarse particulate fraction is the lack of soil fauna at depth that can increase litter surface area via fragmentation (Knowles et al., 2016) and the delivery of labile substrates by creating preferential flow paths. The abundance of bioturbation agents like arthropods generally declines steeply with depth (Jiménez and Decaëns, 2000; Petersen and Luxton, 1982). While there are no earthworms in our soils and faunal abundance was not measured in this experiment, the potential role of bioturbation agents in differentiating litter decomposition processes among depths warrants future study.

Slower root litter decomposition rates may contribute to the older age of native SOC with depth (Hicks Pries et al., 2017b). The effect of slower root litter decomposition with depth is shown in estimates of coarse particulate OC turnover time, which increased from 24 years at 15 cm to 126 years at 95 cm (Table S6). If microbial processing is needed for litter SOC to interact with minerals, mineral interactions will not occur if SOC is stuck in the particulate pool, which may explain why the proportion of SOC that was mineral-associated did not increase with depth in our soils. Furthermore, the old age of mineral-associated SOC with depth may partly be due to the time it takes for coarse particulate matter to be decomposed and become mineral-associated.

The decrease in root decomposition with depth may also explain the increase in C:N ratios and depletion in $\delta^{13}C$ that occurred around 60 cm in our soils. In general, microbial processing of SOC causes C:N ratios to decrease with depth (Rumpel and Kögel-Knabner, 2011), as more C has been respired, and $\delta^{13}C$ to become enriched with depth, as a result of catabolic carboxylation reactions (Ehleringer et al., 2000). However, in our soil, this trend in C:N and $\delta^{13}C$ reverses below 60 cm. Pyrogenic C can have very high C:N ratios (>100; Rajkovich et al., 2012), but the proportion of SOC that was pyrogenic decreased with depth in our soils. Therefore, higher C:N ratios and more depleted $\delta^{13}C$ at depth were likely due to deep SOC being less microbially-processed and more closely resembling the original plant inputs. At depth, the likely source of SOC inputs is roots (Rasse et al., 2005; Schmidt et al., 2011); in the absence of bioturbation, very little leaf and needle-derived organic matter deposited at the surface will move down the soil profile (Hicks Pries et al., 2017a). It remains to be seen whether slower particulate OM decomposition with depth occurs in other soils.

Our results indicate that slower root litter decomposition may contribute to longer residence times of SOC with depth, but that slower root litter decomposition may not be driven by increased organo-mineral associations. Our model results suggest that root litter decomposition may be limited by labile C availability. Particulate SOC at depth could be vulnerable to priming-induced increases in decomposition, if the rate of fresh substrates reaching deep soils increases. Thus, a proportion of deep SOC may be vulnerable to global-change-induced losses if increased precipitation leads to enhanced leaching and transport of DOC from the surface litter. On the other hand, increased root production at depth, if the roots are not actively exuding substrates (Tückmantel et al., 2017), would promote deep SOC storage.

Acknowledgements

This work was supported as part of the Terrestrial Ecosystem Science Program by the Director, Office of Science, Office of Biological and Environmental Research, of the U.S. Department of Energy under Contract No. DE-AC02-05CH11231. We gratefully acknowledge Don Herman for assistance in growing the labeled root litter and for assistance with PLFA analysis at the Firestone Laboratory at UC Berkeley, and the UC Berkeley Center for Forestry Blodgett Forest Research Station for access to and support at the field site.

References

Allison et al., 2009

S.D. Allison, D.S. LeBauer, M.R. Ofrecio, R. Reyes, A.-M. Ta, T.M. Tran**Low levels of nitrogen addition stimulate decomposition by boreal forest fungi**

Soil Biology and Biochemistry, 41 (2009), pp. 293-302

Angst et al., 2016

G. Angst, I. Kögel-Knabner, K. Kirfel, D. Hertel, C.W. Mueller**Spatial distribution and chemical composition of soil organic matter fractions in rhizosphere and non-rhizosphere soil under European beech (Fagus sylvatica L.)**

Geoderma, 264 (2016), pp. 179-187, 10.1016/j.geoderma.2015.10.016

Baldrian, 2017

P. Baldrian**Microbial activity and the dynamics of ecosystem processes in forest soils**

Current Opinion in Microbiology, SI: 37 Environmental microbiology, 37 (2017), pp. 128-134, 10.1016/j.mib.2017.06.008

Beck et al., 1997

T. Beck, R.G. Joergensen, E. Kandeler, F. Makeschin, E. Nuss, H.R. Oberholzer, S. Scheu**An inter-laboratory comparison of ten different ways of measuring soil microbial biomass C**

Soil Biology and Biochemistry, 29 (1997), pp. 1023-1032

Bird et al., 2011

J.A. Bird, D.J. Herman, M.K. Firestone**Rhizosphere priming of soil organic matter by bacterial groups in a grassland soil**

Soil Biology and Biochemistry, 43 (2011), pp. 718-725

Bird and Torn, 2006

J.A. Bird, M.S. Torn**Fine roots vs. needles: a comparison of 13C and 15N dynamics in a ponderosa pine forest soil**

Biogeochemistry, 79 (2006), pp. 361-382

Blagodatskaya and Kuzyakov, 2008

E. Blagodatskaya, Y. Kuzyakov**Mechanisms of real and apparent priming effects and their dependence on soil microbial biomass and community structure: critical review**

Biology and Fertility of Soils, 45 (2008), pp. 115-131, 10.1007/s00374-008-0334-y

Castanha et al., 2018

C. Castanha, B. Zhu, C.E.H. Pries, K. Georgiou, M.S. Torn**The effects of heating, rhizosphere, and depth on root litter decomposition are mediated by soil moisture**

Biogeochemistry, 137 (2018), pp. 267-279

Castellano et al., 2015

M.J. Castellano, K.E. Mueller, D.C. Olk, J.E. Sawyer, J. Six**Integrating plant litter quality, soil organic matter stabilization, and the carbon saturation concept**

Global Change Biology, 21 (2015), pp. 3200-3209

Cotrufo et al., 2015

M.F. Cotrufo, J.L. Soong, A.J. Horton, E.E. Campbell, M.L. Haddix, D.H. Wall, W.J. Parton**Formation of soil organic matter via biochemical and physical pathways of litter mass loss**

Nature Geoscience, 8 (2015), pp. 776-779, 10.1038/ngeo2520

Cotrufo et al., 2013

M.F. Cotrufo, M.D. Wallenstein, C.M. Boot, K. Denef, E. Paul**The Microbial Efficiency-Matrix Stabilization (MEMS) framework integrates plant**

**litter decomposition with soil organic matter stabilization: do labile plant inputs form stable soil organic matter?**

Global Change Biology, 19 (2013), pp. 988-995, 10.1111/gcb.12113

Dashtban et al., 2010

M. Dashtban, H. Schraft, T.A. Syed, W. Qin**Fungal biodegradation and enzymatic modification of lignin**

International Journal of Biochemistry and Molecular Biology, 1 (2010), pp. 36-50

Ehleringer et al., 2000

J.R. Ehleringer, N. Buchmann, L.B. Flanagan**Carbon isotope ratios in belowground carbon cycle processes**

Ecological Applications, 10 (2000), pp. 412-422

Eilers et al., 2012

K.G. Eilers, S. Debenport, S. Anderson, N. Fierer**Digging deeper to find unique microbial communities: the strong effect of depth on the structure of bacterial and archaeal communities in soil**

Soil Biology and Biochemistry, 50 (2012), pp. 58-65, 10.1016/j.soilbio.2012.03.011

Fierer et al., 2003

N. Fierer, J.P. Schimel, P.A. Holden**Variations in microbial community composition through two soil depth profiles**

Soil Biology and Biochemistry, 35 (2003), pp. 167-176, 10.1016/S0038-0717(02)00251-1

Fontaine et al., 2007

S. Fontaine, S. Barot, P. Barré, N. Bdioui, B. Mary, C. Rumpel**Stability of organic carbon in deep soil layers controlled by fresh carbon supply**

Nature, 450 (2007), pp. 277-280

Gabriel and Kellman, 2014

C.-E. Gabriel, L. Kellman**Investigating the role of moisture as an environmental constraint in the decomposition of shallow and deep mineral soil organic matter of a temperate coniferous soil**

Soil Biology and Biochemistry, 68 (2014), pp. 373-384, 10.1016/j.soilbio.2013.10.009

Gill and Burke, 2002

R.A. Gill, I.C. Burke**Influence of soil depth on the decomposition of <Emphasis Type="Italic">Bouteloua gracilis</Emphasis> roots in the shortgrass steppe**

Plant and Soil, 241 (2002), pp. 233-242, 10.1023/A:1016146805542

Gillabel et al., 2010

J. Gillabel, B. Cebrian-Lopez, J. Six, R. Merckx**Experimental evidence for the attenuating effect of SOM protection on temperature sensitivity of SOM decomposition**

Global Change Biology, 16 (2010), pp. 2789-2798, 10.1111/j.1365-2486.2009.02132.x

Gleixner, 2013

G. Gleixner**Soil organic matter dynamics: a biological perspective derived from the use of compound-specific isotopes studies**

Ecological Research, 28 (2013), pp. 683-695, 10.1007/s11284-012-1022-9

Heinze et al., 2018

S. Heinze, B. Ludwig, H.-P. Piepho, R. Mikutta, A. Don, P. Wordell-Dietrich, M. Helfrich, D.Hertel, C. Leuschner, K. Kirfel, E. Kandeler, S. Preusser, G. Guggenberger, T. Leinemann, B. Marschner**Factors controlling the variability of organic matter in the top- and subsoil of a sandy Dystric Cambisol under beech forest**

Geoderma, 311 (2018), pp. 37-44, 10.1016/j.geoderma.2017.09.028

Heitkötter et al., 2017

J. Heitkötter, S. Heinze, B. Marschner**Relevance of substrate quality and nutrients for microbial C-turnover in top- and subsoil of a Dystric Cambisol**

Geoderma, 302 (2017), pp. 89-99, 10.1016/j.geoderma.2017.04.029

Herman et al., 2012

D.J. Herman, M.K. Firestone, E. Nuccio, A. Hodge**Interactions between an arbuscular mycorrhizal fungus and a soil microbial community mediating litter decomposition**

FEMS Microbiology Ecology, 80 (2012), pp. 236-247

Hicks Pries et al., 2017a

C.E. Hicks Pries, J.A. Bird, C. Castanha, P.-J. Hatton, M.S. Torn**Long term decomposition: the influence of litter type and soil horizon on retention of plant carbon and nitrogen in soils**

Biogeochemistry, 134 (2017), pp. 5-16

Hicks Pries et al., 2017b

C.E. Hicks Pries, C. Castanha, R.C. Porras, M.S. Torn**The whole-soil carbon flux in response to warming**

Science, 355 (2017), pp. 1420-1423

Huo et al., 2017

C. Huo, Y. Luo, W. Cheng**Rhizosphere priming effect: a meta-analysis**

Soil Biology and Biochemistry, 111 (2017), pp. 78-84, 10.1016/j.soilbio.2017.04.003

Jenkinson and Coleman, 2008

D.S. Jenkinson, K. Coleman**The turnover of organic carbon in subsoils. Part 2. Modelling carbon turnover**

European Journal of Soil Science, 59 (2008), pp. 400-413, 10.1111/j.1365-2389.2008.01026.x

Jiang et al., 2014

X. Jiang, L. Cao, R. Zhang, L. Yan, Y. Mao, Y. Yang**Effects of nitrogen addition and litter properties on litter decomposition and enzyme activities of individual fungi**

Applied Soil Ecology, 80 (2014), pp. 108-115, 10.1016/j.apsoil.2014.04.002

Jiménez and Decaëns, 2000

J.J. Jiménez, T. Decaëns**Vertical distribution of earthworms in grassland soils of the Colombian Llanos**

Biology and Fertility of Soils, 32 (2000), pp. 463-473, 10.1007/s003740000277

Jobbágy and Jackson, 2000

E.G. Jobbágy, R.B. Jackson**The vertical distribution of soil organic carbon and its relation to climate and vegetation**

Ecological Applications, 10 (2000), pp. 423-436

Joergensen and Mueller, 1996

R.G. Joergensen, T. Mueller**The fumigation-extraction method to estimate soil microbial biomass: calibration of the kEN value**

Soil Biology and Biochemistry, 28 (1996), pp. 33-37, 10.1016/0038-0717(95)00101-8

Karhu et al., 2016

K. Karhu, E. Hilasvuori, H. Fritze, C. Biasi, H. Nykänen, J. Liski, P. Vanhala, J. Heinonsalo, J.Pumpanen**Priming effect increases with depth in a boreal forest soil**

Soil Biology and Biochemistry, 99 (2016), pp. 104-107, 10.1016/j.soilbio.2016.05.001

Keeler et al., 2009

B.L. Keeler, S.E. Hobbie, L.E. Kellogg**Effects of long-term nitrogen addition on microbial enzyme activity in eight forested and grassland sites: implications for litter and soil organic matter decomposition**

Ecosystems, 12 (2009), pp. 1-15

Knorr et al., 2005

M. Knorr, S.D. Frey, P.S. Curtis**Nitrogen additions and litter decomposition: a meta-analysis**

Ecology, 86 (2005), pp. 3252-3257

Knowles et al., 2016

M.E. Knowles, D.S. Ross, J.H. Görres**Effect of the endogeic earthworm Aporrectodea tuberculata on aggregation and carbon redistribution in uninvaded forest soil columns**

Soil Biology and Biochemistry, 100 (2016), pp. 192-200, 10.1016/j.soilbio.2016.06.016

Kögel-Knabner et al., 2008

I. Kögel-Knabner, G. Guggenberger, M. Kleber, E. Kandeler, K. Kalbitz, S. Scheu, K.Eusterhues, P. Leinweber**Organo-mineral associations in temperate soils: integrating biology, mineralogy, and organic matter chemistry**

Journal of Plant Nutrition and Soil Science, 171 (2008), pp. 61-82, 10.1002/jpln.200700048

Koven et al., 2013

C.D. Koven, W.J. Riley, A. Stern**Analysis of permafrost thermal dynamics and response to climate change in the CMIP5 Earth System Models**

Journal of Climate, 26 (2013), pp. 1877-1900

Kramer and Gleixner, 2008

C. Kramer, G. Gleixner**Soil organic matter in soil depth profiles: distinct carbon preferences of microbial groups during carbon transformation**

Soil Biology and Biochemistry, 40 (2008), pp. 425-433

Kuzyakov, 2010

Y. Kuzyakov**Priming effects: interactions between living and dead organic matter**

Soil Biology and Biochemistry, 42 (2010), pp. 1363-1371, 10.1016/j.soilbio.2010.04.003

Lavelle, 1988

P. Lavelle**Earthworm activities and the soil system**

Biology and Fertility of Soils, 6 (1988), pp. 237-251

Lavelle et al., 2006

P. Lavelle, T. Decaëns, M. Aubert, S. Barot, M. Blouin, F. Bureau, P. Margerie, P. Mora, J.-P.Rossi**Soil invertebrates and ecosystem services**

European Journal of Soil Biology, 42 (2006), pp. S3-S15

Lenth, 2016

R.V. Lenth**Least-squares means: the R package lsmeans | lenth**

Journal of Statistical Software (2016), 10.18637/jss.v069.i01

Mathieu et al., 2015

J.A. Mathieu, C. Hatté, J. Balesdent, É. Parent**Deep soil carbon dynamics are driven more by soil type than by climate: a worldwide meta-analysis of radiocarbon profiles**

Global Change Biology, 21 (2015), pp. 4278-4292, 10.1111/gcb.13012

Petersen and Luxton, 1982

H. Petersen, M. Luxton**A comparative analysis of soil fauna populations and their role in decomposition processes**

Oikos, 39 (1982), pp. 288-388, 10.2307/3544689

Phillips et al., 2011

R.P. Phillips, A.C. Finzi, E.S. Bernhardt**Enhanced root exudation induces microbial feedbacks to N cycling in a pine forest under long-term CO2 fumigation**

Ecology Letters, 14 (2011), pp. 187-194

Preusser et al., 2017

S. Preusser, S. Marhan, C. Poll, E. Kandeler**Microbial community response to changes in substrate availability and habitat conditions in a reciprocal subsoil transfer experiment**

Soil Biology and Biochemistry, 105 (2017), pp. 138-152, 10.1016/j.soilbio.2016.11.021

R Development Core Team, 2017

R Development Core Team**R: a Language and Environment for Statistical Computing**

R Foundation for Statistical Computing, Vienna, Austria (2017)

Rajkovich et al., 2012

S. Rajkovich, A. Enders, K. Hanley, C. Hyland, A.R. Zimmerman, J. Lehmann**Corn growth and nitrogen nutrition after additions of biochars with varying properties to a temperate soil**

Biology and Fertility of Soils, 48 (2012), pp. 271-284

Rasmussen et al., 2005

C. Rasmussen, M.S. Torn, R.J. Southard**Mineral assemblage and aggregates control carbon dynamics in a California conifer forest**

Soil Science Society of America Journal, 69 (2005), pp. 1711-1721

Rasse et al., 2005

D.P. Rasse, C. Rumpel, M.-F. Dignac**Is soil carbon mostly root carbon? Mechanisms for a specific stabilisation**

Plant and Soil, 269 (2005), pp. 341-356, 10.1007/s11104-004-0907-y

Rumpel et al., 2010

C. Rumpel, K. Eusterhues, I. Kögel-Knabner**Non-cellulosic neutral sugar contribution to mineral associated organic matter in top-and subsoil horizons of two acid forest soils**

Soil Biology and Biochemistry, 42 (2010), pp. 379-382

Rumpel and Kögel-Knabner, 2011

C. Rumpel, I. Kögel-Knabner**Deep soil organic matter—a key but poorly understood component of terrestrial C cycle**

Plant and Soil, 338 (2011), pp. 143-158

Rumpel et al., 2002

C. Rumpel, I. Kögel-Knabner, F. Bruhn**Vertical distribution, age, and chemical composition of organic carbon in two forest soils of different pedogenesis**

Organic Geochemistry, 33 (2002), pp. 1131-1142

Salomé et al., 2010

C. Salomé, N. Nunan, V. Pouteau, T.Z. Lerch, C. Chenu**Carbon dynamics in topsoil and in subsoil may be controlled by different regulatory mechanisms**

Global Change Biology, 16 (2010), pp. 416-426, 10.1111/j.1365-2486.2009.01884.x

Sanaullah et al., 2011

M. Sanaullah, A. Chabbi, J. Leifeld, G. Bardoux, D. Billou, C. Rumpel**Decomposition and stabilization of root litter in top-and subsoil horizons: what is the difference?**

Plant and Soil, 338 (2011), pp. 127-141

Schmidt et al., 2011

M.W. Schmidt, M.S. Torn, S. Abiven, T. Dittmar, G. Guggenberger, I.A. Janssens, M. Kleber, I. Kögel-Knabner, J. Lehmann, D.A. Manning, others**Persistence of soil organic matter as an ecosystem property**

Nature, 478 (2011), pp. 49-56

Schrumpf et al., 2013

M. Schrumpf, K. Kaiser, G. Guggenberger, T. Persson, I. Kögel-Knabner, E.-D. Schulze**Storage and stability of organic carbon in soils as related to depth, occlusion within aggregates, and attachment to minerals**

Biogeosciences, 10 (2013), pp. 1675-1691

Silver and Miya, 2001

W.L. Silver, R.K. Miya**Global patterns in root decomposition: comparisons of climate and litter quality effects**

Oecologia, 129 (2001), pp. 407-419, 10.1007/s004420100740

Six et al., 2004

J. Six, H. Bossuyt, S. Degryze, K. Denef**A history of research on the link between (micro) aggregates, soil biota, and soil organic matter dynamics**

Soil and Tillage Research, 79 (2004), pp. 7-31

Soil Science Division Staff, 2017

Soil Science Division Staff**Soil survey manual**

C. Ditzler, K. Scheffe, H.C. Monger (Eds.), USDA Handbook 18, Government Printing Office, Washington, D.C (2017)

Solly et al., 2015

E.F. Solly, I. Schöning, N. Herold, S.E. Trumbore, M. Schrumpf**No depth-dependence of fine root litter decomposition in temperate beech forest soils**

Plant and Soil, 393 (2015), pp. 273-282, 10.1007/s11104-015-2492-7

Stewart et al., 2008

C.E. Stewart, K. Paustian, R.T. Conant, A.F. Plante, J. Six**Soil carbon saturation: evaluation and corroboration by long-term incubations**

Soil Biology and Biochemistry, 40 (2008), pp. 1741-1750

Sulman et al., 2017

B.N. Sulman, E.R. Brzostek, C. Medici, E. Shevliakova, D.N.L. Menge, R.P. Phillips**Feedbacks between plant N demand and rhizosphere priming depend on type of mycorrhizal association**

Ecology Letters, 20 (2017), pp. 1043-1053, 10.1111/ele.12802

Sulman et al., 2014

B.N. Sulman, R.P. Phillips, A.C. Oishi, E. Shevliakova, S.W. Pacala**Microbe-driven turnover offsets mineral-mediated storage of soil carbon under elevated CO 2**

Nature Climate Change, 4 (2014), p. 1099

Swanston et al., 2005

C.W. Swanston, M.S. Torn, P.J. Hanson, J.R. Southon, C.T. Garten, E.M. Hanlon, L. Ganio**Initial characterization of processes of soil carbon stabilization using forest stand-level radiocarbon enrichment**

Geoderma, Mechanisms and regulation of organic matter stabilisation in soils, 128 (2005), pp. 52-62, 10.1016/j.geoderma.2004.12.015

Tian et al., 2016

Q. Tian, X. Yang, X. Wang, C. Liao, Q. Li, M. Wang, Y. Wu, F. Liu**Microbial community mediated response of organic carbon mineralization to labile carbon and nitrogen addition in topsoil and subsoil**

Biogeochemistry, 128 (2016), pp. 125-139, 10.1007/s10533-016-0198-4

Tückmantel et al., 2017

T. Tückmantel, C. Leuschner, S. Preusser, E. Kandeler, G. Angst, C.W. Mueller, I.C.Meier**Root exudation patterns in a beech forest: dependence on soil depth, root morphology, and environment**

Soil Biology and Biochemistry, 107 (2017), pp. 188-197, 10.1016/j.soilbio.2017.01.006

Vance et al., 1987

E.D. Vance, P.C. Brookes, D.S. Jenkinson**An extraction method for measuring soil microbial biomass C**

Soil Biology and Biochemistry, 19 (1987), pp. 703-707, 10.1016/0038-0717(87)90052-6

Vogel et al., 2014

C. Vogel, C.W. Mueller, C. Höschen, F. Buegger, K. Heister, S. Schulz, M. Schloter, I. Kögel-Knabner**Submicron structures provide preferential spots for carbon and nitrogen sequestration in soils**

Nature Communications, 5 (2014), p. 2947, 10.1038/ncomms3947

White and Ringelberg, 1998

D.C. White, D.B. Ringelberg**Signature lipid biomarker analysis**

Techniques in Microbial Ecology, 1 (1998), pp. 255-272

Wiedemeier et al., 2013

D.B. Wiedemeier, M.D. Hilf, R.H. Smittenberg, S.G. Haberle, M.W. Schmidt**Improved assessment of pyrogenic carbon quantity and quality in environmental samples by high-performance liquid chromatography**

Journal of Chromatography A, 1304 (2013), pp. 246-250

Wiedemeier et al., 2016

D.B. Wiedemeier, S.Q. Lang, M. Gierga, S. Abiven, S.M. Bernasconi, G.L. Früh-Green, I. Hajdas, U.M. Hanke, M.D. Hilf, C.P. McIntyre, M.P.W. Scheider, R.H. Smittenberg, L. Wacker, G.L.B.Wiesenberg, M.W.I. Schmidt**Characterization, quantification and compound-specific isotopic analysis of pyrogenic carbon using benzene polycarboxylic acids (BPCA)**

Journal of Visualized Experiments: Journal of Visualized Experiments (2016), 10.3791/53922

Wordell-Dietrich et al., 2017

P. Wordell-Dietrich, A. Don, M. Helfrich**Controlling factors for the stability of subsoil carbon in a Dystric Cambisol. Geoderma**

5th International Symposium on Soil Organic Matter 2015 (2017), pp. 40-48, 10.1016/j.geoderma.2016.08.023

304

Zelles, 1999

L. Zelles**Fatty acid patterns of phospholipids and lipopolysaccharides in the characterisation of microbial communities in soil: a review**

Biol. Fertil. Soils, 29 (1999), pp. 111-129

Zogg et al., 1997

G.P. Zogg, D.R. Zak, D.B. Ringelberg, D.C. White, N.W. MacDonald, K.S. Pregitzer**Compositional and functional shifts in microbial communities due to soil warming**

Soil Sci. Soc. Am. J., 61 (1997), pp. 475-481

Zuur et al., 2009

A. Zuur, E.N. Ieno, N. Walker, A.A. Saveliev, G.M. Smith, *et al.***Mixed Effects Models and Extensions in Ecology with R**

(2009 edition), Springer, New York, NY (2009)